Published in final edited form as:

Nature. 2017 September 14; 549(7671): 282–286. doi:10.1038/nature23676.

The neuropeptide Neuromedin U stimulates innate lymphoid cells and type 2 inflammation

Christoph S.N. Klose[1], **Tanel Mahlakõiv**[1], **Jesper B. Moeller**[1,2], **Lucille C. Rankin**[1], **Anne-Laure Flamar**[1], **Hiroki Kabata**[1], **Laurel A. Monticelli**[1], **Saya Moriyama**[1], **Gregory Garbès Putzel**[1], **Nikolai Rakhilin**[3,4], **Xiling Shen**[3,4], **Evi Kostenis**[5], **Gabriele M. König**[5], **Takashi Senda**[6,7], **Dustin Carpenter**[6,7], **Donna L. Farber**[6,7], and **David Artis**[1,*]

[1]Jill Roberts Institute for Research in Inflammatory Bowel Disease, Joan and Sanford I. Weill Department of Medicine, Department of Microbiology and Immunology, Weill Cornell Medicine, Cornell University, New York, NY 10021, USA

[2]Institute of Molecular Medicine, University of Southern Denmark, 5000 Odense, Denmark

[3]Department of Biomedical Engineering, Duke University, Durham, NC 27708, USA

[4]School of Electrical and Computer Engineering, Cornell University, Ithaca, NY 14853, USA

[5]Institute of Pharmaceutical Biology, University of Bonn, 53115 Bonn, Germany

[6]Columbia Center for Translational Immunology and Department of Microbiology and Immunology, Columbia University Medical Center, New York, NY 10032, USA

[7]Department of Surgery, Columbia University Medical Center, New York, NY 10032, USA

Abstract

The type 2 cytokines interleukin (IL)-4, IL-5, IL-9 and IL-13 play critical roles in stimulating innate and adaptive immune responses required for resistance to helminth infection and promotion of allergic inflammation, metabolic homeostasis and tissue repair[1–3]. Group 2 innate lymphoid cells (ILC2s) are a potent source of type 2 cytokines and while significant advances have been made in understanding the cytokine milieu that promotes ILC2 responses[4–9], there are fundamental gaps in knowledge regarding how ILC2 responses are regulated by other stimuli. In this report, we demonstrate that ILC2s in the gastrointestinal tract co-localize with cholinergic

[*]**Corresponding author:** David Artis, Ph.D. Weill Cornell Medicine, Cornell University, Joan and Sanford I. Weill Department of Medicine, Belfer Research Building, Room 724 (box 210), 413 East 69th Street, New York, NY 10021, USA, Tel: 1-646-962-6291, dartis@med.cornell.edu.

Authorship contributions

C.S.N.K. carried out most experiments and analyzed the data. T.M., J.B.M., L.C.R., A.-L.F., H.K., L.A.M., S.M., N.R. and X.S. helped with experiments and E.K. and G.M.K provided the inhibitor FR900359 (previous commercial name UBO-QIC). G.G.P. performed RNA-seq analysis. T.S., D.C. and D.L.F. provided human tissue samples. D.A. and C.S.N.K. conceived the project, analyzed data, and wrote the manuscript with input from all co-authors.

Disclosure of conflicts of interest

The authors declare no competing conflict of interest.

Data availability

RNA-seq data are deposited as GSE101625 in the Gene Expression Omnibus database.

neurons that express the neuropeptide neuromedin U (NMU)[10,11]. In contrast to other hematopoietic cells, ILC2s selectively express the NMU receptor 1 (NMUR1). *In vitro* stimulation of ILC2s with NMU induced rapid cell activation, proliferation and secretion of type 2 cytokines IL-5, IL-9 and IL-13 that was dependent on cell-intrinsic expression of NMUR1 and Gαq protein. *In vivo* administration of NMU triggered potent type 2 cytokine responses characterized by ILC2 activation, proliferation and eosinophil recruitment that was associated with accelerated expulsion of the gastrointestinal nematode *Nippostrongylus brasiliensis* or induction of lung inflammation. Conversely, worm burden was higher in *Nmur1*$^{-/-}$ mice compared to control mice. Further, use of gene-deficient mice and adoptive cell transfer experiments revealed that ILC2s were necessary and sufficient to mount NMU-elicited type 2 cytokine responses. Together, these data indicate that the NMU-NMUR1 neuronal signaling circuit provides a selective and previously unrecognized mechanism through which the enteric nervous system and innate immune system integrate to promote rapid type 2 cytokine responses that can induce anti-microbial, inflammatory and tissue-protective type 2 responses at mucosal sites.

In addition to being populated by cells of the innate and adaptive immune systems, mucosal sites are heavily innervated[12,13]. Immunofluorescence staining of the neuronal marker SNAP-25 together with the ILC2 marker KLRG1[14] and CD3ε revealed that ILC2s and T cells were closely associated with SNAP-25^{+} neurons in the intestine (Fig. 1a). Surface reconstruction suggested that neurons and ILC2s form close inter-cellular contacts (Extended Data (ED) 1). To test whether neuron-derived signals might be sensed by ILC2s, we performed RNA-seq and KEGG pathway analysis of ILC subsets. Multiple genes associated with neuroactive-receptor-ligand-interactions were differentially expressed between ILC2s and ILC3s (Fig. 1b). The most differentially expressed gene in ILC2s in this category was *Nmur1*, a receptor for the neuropeptide NMU, which has previously been reported to provoke anorexic effects in the central nervous system and promote cutaneous inflammation[10,11,15,16]. We compared *Nmur1* expression to several highly differentially expressed genes found in ILC3s (*Rorc*, *Il17f*, *Il1r1* and *Il22*) or in ILC2s (*Gata3* and *Il1rl1*). *Nmur1* expression segregated in ILC2s to a comparable degree to that noted for other ILC2-associated genes (Fig. 1c). The selective expression of *Nmur1* in ILC2s but not in other innate and adaptive lymphocyte lineages or myeloid cells was confirmed by qPCR analysis (Fig. 1d; ED 2a). In contrast, a second receptor for NMU (*Nmur2*), which is predominately expressed in the central nervous system[10,11], was not detected in any of the immune cell populations examined (Fig. 1c,d). Expression of *NMUR1* was also detectable in human intestinal ILCs but not in B cells suggesting that human ILCs sense neuronal signals via NMUR1 (Fig. 1e).

Analysis of NMUR1 protein expression using a LacZ reporter revealed that 2% of all CD45^{+} cells in the small intestine were NMUR1^{+} in *Nmur1*$^{LacZ/+}$ but not in control *Nmur1*$^{+/+}$ mice that lacked the reporter (Fig. 1f). Analysis of NMUR1^{+} cells revealed that 96% of NMUR1^{+} cells were negative for cell lineage markers such as CD3, CD5, FcεRI, CD11b, CD11c and B220 but expressed the ILC2 markers CD127 and KLRG1 (Fig. 1f). Consistent with mRNA expression, ILC2s expressed *LacZ* under the control of the *Nmur1* promoter, while no expression was detected in B cells, T cells, ILC1s, ILC3s, eosinophils, mast cells, macrophages and basophils (ED 2b-g). Thus, *Nmur1* is selectively expressed in ILC2s.

The ligand of NMUR1 is the 23 amino acid long neuropeptide NMU[10,11]. *Nmu* was not detectable by qPCR in the epithelial or lamina propria fractions of the small intestine isolated from mouse or human specimens but was expressed in the parenchymal tissue of the small intestine, suggesting that hematopoietic cells do not express NMU (ED 2h,i). Immunofluorescence staining of intestinal tissue or use of Nmu^{Gfp} reporter mice revealed a network of NMU^{+} neurons including the plexus myentericus, plexus submucosus and nerve fibers that are located below the tips of the villi (Fig. 1g; ED 2j-l). Notably, NMU was expressed in cholinergic (marked by choline acetyl-transferase (Chat) expression) but not in catecholaminergic neurons (marked by tyrosine hydroxylase (TH) expression) (Fig. 1h; ED 2m). NMU^{+} neurons co-localized with ILC2s and 68% of ILC2s had overlapping pixels with neurons (Fig. 1i; ED 3a,b). Further, co-culture of ILC2s together with enteric neurons that expressed NMU led to increased proliferation and blasting of ILC2s suggesting that enteric nerve-derived bioactive factors directly activate ILC2s (ED 3c-e). Together, these data indicate that NMUR1 is specifically expressed by ILC2s, which co-localize with NMU^{+} cholinergic neurons in the intestine and that ILC2s might sense nerve-derived signals.

To test whether NMU stimulates ILC2s, we isolated lamina propria lymphocytes (LPLs) from IL-13 reporter mice[17] and incubated them *in vitro* with or without NMU. NMU potently activated ILC2s as measured by IL-13 expression (Fig. 2a,b; ED 4a). We confirmed the capacity of NMU to induce IL-5 and IL-13 production by intracellular cytokine staining (Fig. 2c,d) and ELISA (ED 4b,c). Further, a comparison of stimulation of ILC2s with NMU versus combinations of IL-2, IL-7, IL-25 and IL-33 or PMA and ionomycin (all stimuli known to stimulate ILC2s[14,18–20]), revealed that NMU-induced expression of IL-5 and IL-13 in ILC2s was stronger than the effects of cytokines previously known to activate ILC2s. Indeed, only a combination of IL-2, IL-7, IL-25 and IL-33 or PMA and ionomycin stimulation resulted in comparable ILC2 activation as NMU stimulation (Fig. 2e,f). Since NMU could trigger potent cytokine production from ILC2s lacking IL-33 responsiveness, we conclude that NMU can activate ILC2s independently of IL-33 (ED 4d).

In order to investigate whether NMU activation of ILC2s requires NMUR1 we examined $Nmur1^{-/-}$ mice. ILC2s developed in comparable proportions in $Nmur1^{-/-}$ mice and did not exhibit obvious defects at steady-state (ED 4e,f). However, only ILC2s from $Nmur1^{+/+}$ but not from $Nmur1^{-/-}$ mice were activated by NMU to produce type 2 cytokines (Fig. 2g). In contrast, ILC2s from both genotypes could be activated by PMA and ionomycin demonstrating that ILC2s from $Nmur1^{-/-}$ were responsive to stimulation but had a specific defect in the NMUR1 signaling pathway (Fig. 2g). In addition, chemical inhibition of Gαq family of proteins, which mediate NMUR1 signal transduction[21], completely abolished activation of ILC2s but had only modest effects on ILC2 stimulation with IL-2, IL-7, IL-25 and IL-33 (Fig. 2h; ED 4g). Thus, NMU appears to trigger a NMUR1- and Gαq-dependent signaling pathway in ILC2s.

To test whether the stimulation of NMUR1 signaling by NMU is ILC2-intrinsic, we isolated LPLs from CD45.1 $Nmur1^{+/+}$: CD45.2 $Nmur1^{-/-}$ mixed bone marrow chimeras and stimulated them *in vitro* with NMU or PMA and ionomycin. Only CD45.1 $Nmur1^{+/+}$ ILC2s but not CD45.2 $Nmur1^{-/-}$ ILC2s expressed IL-5 and IL-13 following NMU stimulation, whereas ILC2s from both genotypes were activated by PMA and ionomycin (ED 4h). In

addition, NMU stimulation of sort-purified ILC2s resulted in blasting and a significant increase in IL-5, IL-9 and IL-13 production as measured by flow cytometry or by Legendplex bead-based assay (Fig. 2i-m; ED 4i-l). Therefore, we conclude that NMU promotes type 2 cytokine production from ILC2s through activating NMUR1 on ILC2s.

To further elucidate the pathways activated in ILC2s by NMU stimulation, we sort-purified ILC2s from PBS- or NMU-treated mice and performed transcriptional profiling by RNA-seq. Transcripts from PBS- and NMU-treated ILC2s clustered separately (Fig. 3a) and GO-term analysis revealed that NMU activates processes related to cell cycle regulation and cell division (Fig. 3b), including expression of the cell cycle-associated genes *Kntc1*, *Chaf1a*, *Cdc6*, *Spag5*, *Brca1*, *Mki67* and *Cdca3* (Fig. 3c). Flow cytometric analysis for Ki67, the protein encoded by *MKi67*, demonstrated that NMU administration resulted in significantly increased proliferation of ILC2s but not of ILC3s (Fig. 3d,e; ED 5a). Injection of NMU into CD45.1 *Nmur1*$^{+/+}$: CD45.2 *Nmur1*$^{-/-}$ mixed bone marrow chimeras revealed an ILC2-intrinsic requirement for NMUR1 to respond to NMU *in vivo* (Fig. 3f; ED 5b-d). In addition, *in vivo* delivery of NMU induced blasting (ED 5e) and maturation (Fig. 3g) of ILC2s that was associated with prototypic type 2 inflammation marked by production of IL-13 (Fig. 3h,i) and goblet cell hyperplasia (Fig. 3j,k).

Since the intestine is highly innervated by a network of NMU^{+} neurons (Fig. 1i), we investigated the role of NMU in immunity to the helminth parasite *Nippostrongylus brasiliensis* (*N. brasiliensis*), an intestinal parasite infection model, in which immunity is critically dependent on activation of ILC2s[17,22,23]. Consistent with a role for NMU in regulating ILC2 responses during helminth infection, *Nmu* expression was up-regulated following infection with *N. brasiliensis* and was a conserved response following exposure to the related nematode parasites *Trichuris muris* (*T. muris*) and *Heligmosomoides polygyrus* (*H. polygyrus*) (Fig. 3l; ED 5f,g). Since NMUR1 is specifically expressed on ILC2s at steady-state (Fig. 1d,f,; ED 2b-g), we sought to test whether NMUR1 is induced on other cell types following exposure to *N. brasiliensis* infection. Although increased Nmur1 expression was detected on ILC2s (ED 5h), Nmur1 expression was still specific for ILC2s and not detected on sizable proportions of other immune cell populations including mast cells, basophils, macrophages, T cells or IL-4-producing Th2 cells, indicating that NMU is not acting directly on other hematopoietic cells (Fig. 3m; ED 5i-l). However, in order to rule out that some of the effects of NMU *in vivo* require mast cell or eosinophils, in which *Nmur1* was detected in previous publications[15,24], we injected NMU in mast cell-deficient or eosinophil-deficient mice. Consistent with *Nmur1* expression results, NMU elicited potent ILC2 activation in mast-cell-deficient *Cpa3*$^{Cre/+}$ and eosinophil-deficient ΔdblGATA1 mice, demonstrating that ILC2 activation by NMU is independent of eosinophils and mast cells *in vivo* (ED 5m-o).

Delivery of NMU following *N. brasiliensis* infection was associated with elevated eosinophilia and accelerated worm expulsion (Fig. 3n,o). *N. brasiliensis*-infected *Nmur1*-deficient mice and *Nmur1*$^{-/-}$ bone marrow chimeras exhibited elevated worm burden and reduced ILC2 responses (Fig. 3p,q; ED 5p). To test whether there is a cell-intrinsic role for NMUR1 on ILC2s, we reconstituted *Rag2*$^{-/-}$ *Il2rg*$^{-/-}$ mice with ILC2 progenitors (ILC2p) derived from either *Nmur1*$^{+/+}$ or *Nmur1*$^{-/-}$ mice. Accelerated worm expulsion and increased

ILC2 numbers were observed in recipients reconstituted with *Nmur1*$^{+/+}$ ILC2ps compared to those reconstituted with *Nmur1*$^{-/-}$ ILC2ps (Fig. 3r,s). Administration of NMU to *Rag2*$^{-/-}$ *Il2rg*$^{-/-}$ mice reconstituted with ILC2ps derived from either *Nmur1*$^{+/+}$ or *Nmur1*$^{-/-}$ mice resulted in an enhanced worm expulsion and type 2 response in mice reconstituted with *Nmur1*$^{+/+}$ precursors, indicating that NMU stimulates ILC2s *in vivo* and promotes ILC2-dependent immunity to infection (Fig. 3t-v; ED 5q).

To investigate whether NMU can influence ILC2 responses at other mucosal barriers we delivered NMU intranasally. NMU administration stimulated maturation, cytokine expression and proliferation of lung ILC2s (Fig. 4a-c; ED 6a). Associated with this, NMU administration resulted in increased eosinophilia in bronchoalveolar lavage (BAL) and lung tissue and enhanced mucus production compared to PBS-treated control animals (Fig. 4d,e; ED 6b). To directly test whether NMU-induced lung inflammation is dependent on ILC2s, NMU was administered to ILC2-sufficient *Rag2*$^{-/-}$ versus ILC2-deficient *Rag2*$^{-/-}$ *Il2rg*$^{-/-}$ mice. NMU administration to *Rag2*$^{-/-}$ mice resulted in robust ILC2 activation, eosinophil recruitment and airway inflammation compared to PBS-treated *Rag2*$^{-/-}$ mice, while no recruitment of eosinophils was observed in *Rag2*$^{-/-}$ *Il2rg*$^{-/-}$ mice (Fig. 4f,g; ED 6c). Reconstitution of *Rag2*$^{-/-}$ *Il2rg*$^{-/-}$ mice with ILC2ps[14] restored ILC2 populations in the lung (ED 6d) and delivery of NMU resulted in robust ILC2 proliferation and eosinophilia that was absent in ILC2-deficient recipients (Fig. 4h,i). Lastly, delivery of NMU to *Nmur1*$^{+/+}$ or *Nmur1*$^{-/-}$ mice demonstrated the requirement for *Nmur1* in eliciting NMU-dependent ILC2 responses *in vivo* (Fig. 4j,k; ED 6e).

Taken together, these findings elaborate a new pathway that enables neuronal-immune system cross-talk and identify a previously unrecognized role for cholinergic neuron-derived NMU in promoting activation, proliferation and effector functions of ILC2s at mucosal sites. The discovery that NMU can promote ILC2 responses and accelerate type 2 inflammation provokes the hypothesis that beyond their capacity to respond to cytokines and alarmins, ILC2s may have selectively co-evolved with the enteric nervous system to coordinate early sensing and responsiveness to infectious and foreign stimuli at barrier surfaces. We propose that cholinergic enteric neuron-derived neuromedin U functions as a neuronal amplifier that primes ILC2s for rapid and optimal activation by promoting their entry into cell cycle or their responsiveness to other host-derived or environmental stimuli, which are essential activation and/or survival factors for ILC2s. Moreover, the appreciation that the immediate response capability of the nervous system can elicit a strong, rapid and selective activation of ILC2s provides new insights into the pathophysiology of innate type 2 cytokine responses associated with exposure to multiple infectious agents, environmental allergens and pollutants at mucosal sites.

Experimental Procedures

Mouse strains

C57BL/6 mice and CD45.1 mice on C57BL/6 background (B6.SJL-Ptprca Pepcb/BoyJ) were purchased from The Jackson Laboratory. *Rag2*$^{-/-}$ and *Rag2*$^{-/-}$ *Il2rg*$^{-/-}$ on a C57BL/6 background were from Taconic Farms. *Chat*^{Gfp} [25], *Chat*^{Cre} [26], Ai14 [27], *Id2*^{Gfp} [28] on a C57BL/6 background and *Il13*$^{Yfp/+}$ [17], *Il4*^{Gfp} [29] and ΔdblGATA1[30] on a BALB/c

background were originally from The Jackson Laboratory. These strains, together with *Cpa3*^{Cre} [31], *Il1rl1*$^{-/-}$ [32] and the strains mentioned below, were bred at Weill Cornell Medicine. *Nmur1*$^{LacZ/+}$ (*Nmur1*$^{tm1.1(KOMP)Vlcg}$) were generated by Velocigene using C57BL/6 ES cells in which the *Nmur1* gene was replaced by *LacZ* and a floxed neomyin cassette. The neomycin cassette was removed by crossing the mice to Cre deleter mice. Breeding of *Nmur1*$^{LacZ/+}$ to homozygosity resulted in *Nmur1-deficient (Nmur1*$^{LacZ/LacZ}$) *mice* referred to as *Nmur1*$^{-/-}$. *Nmu*^{Gfp} were generated by Gensat and provided on a Swiss Webster background. Sex and age-matched animals between 6 and 16 weeks of age were used for experiments if not otherwise indicated. We did not use randomization to assign animals to experimental groups. Investigators were not blinded to group allocation during experiments. No animals were excluded from the analysis unless clearly indicated. All animal experiments were approved and are in accordance with the Institutional Animal Care and Use Committee guidelines at Weill Cornell Medicine.

Isolation of cells from the lamina propria and the lung

Small intestine was removed, cleaned from remaining fat tissue and washed in ice-cold PBS (Corning). Peyer's patches were identified and eliminated. Small intestine was opened longitudinally and washed in ice-cold PBS. Dissociation of epithelial cells was performed by incubation on a shaker at 37°C in HBSS (Sigma-Aldrich) containing 10 mM Hepes and 5 mM EDTA (both Thermo Fisher Scientific) or 1mM DTT (Sigma-Aldrich) two times for 15 min. After each step, samples were vortexed and the epithelial fraction discarded. Afterwards, remaining tissue was chopped into small pieces and enzymatic digestion was performed using Dispase (5 U/ml; Thermo Fisher Scientific), Collagenase III (1 mg/ml; Worthington) and DNaseI (20 μg/ml; Sigma-Aldrich). Leukocytes were further enriched by a 40%/80% Percoll gradient centrifugation (Sigma-Aldrich).

One PBS-perfused lung lobe was minced and incubated using same conditions and enzymatic cocktail as for the intestine for 45 min at 37°C. Afterwards lung was vortexed, mashed through a 70 μM cell strainer and purified over a 40%/80% Percoll gradient.

Mesenteric lymph nodes were chopped and incubated in RPMI medium supplemented with 1% BSA (Sigma-Aldrich), DNaseI (20 μg/ml) and Collagenase II (1 mg/ml; Sigma-Aldrich) for 20 min at 37°C. Specimens were mechanically dissociated and filtered through a 70 μM cell strainer.

Flow cytometry and cell sorting

After saturating the Fc-receptors with CD16/CD32 blocking antibody (Biolegend), single cell suspensions were incubated on ice with conjugated antibodies in PBS (Ca^{2+} and Mg^{2+}-free). Dead cells were routinely excluded with Fixable Aqua Dead Cell Stain or SYTOX Blue Dead Cell Stain (Thermo Fisher Scientific). Lineage-positive cells were excluded by staining for CD3ε (145-2C11), CD5 (53-7.3), FcεRI (Mar-1), B220 (RA3-6B2), CD11b (M1/70) and CD11c (N418). For surface staining KLRG1 (2F1), CD45 (30-F11), CD45.1 (A20), CD45.2 (104), CD25 (PC61), CD127 (A7R34), SiglecF (E50-2440), CCR6 (29-2L17), NKp46 (29A1.4), NK1.1 (PK136), c-kit (2B8), CD49b (HMα2), CD19 (eBio1D3), CD90.2 (53-2.1), ST2 (DIH9) and F4/80 (BM8) were used. Intracellular staining

with IL-5 (TRFK5) and IL-13 (eBIO13A) antibodies was carried out by using the Cytofix/Cytoperm Fixation/Permeabalization Solution and Perm/Wash bufffer (BD Biosciences). GATA-3 (TWAJ), RORγt (B2D) and Ki67 (B56) were stained using the Foxp3 transcription factor staining buffer set (eBioscience). Human ILCs were sort-purified as $CD45^+$ (HI30), $CD3\varepsilon^-$ (UCHT1), $CD5^-$ (UCHT2), $CD19^-$ (HIB19), $CD11b^-$ (CBRM1/5), $CD11c^-$ (3.9) $CD14^-$ (HCD14) and $CD127^+$ (eBioRDR5) cells. All antibodies used in flow cytometry were purchased from eBioscience, Biolegend or BD Biosciences. LacZ was visualized by using the FluoReporter lacZ Flow Cytometry Kit according to the manufacture's protocol (Thermo Fisher Scientific) and 2 min incubation time. All flow cytometry experiments were acquired using a custom configuration Fortessa flow cytometer and the FACS Diva software (BD Biosciences) and analyzed with FlowJo V9.9.3 software (TreeStar) or sort-purified by using a custom configuration FACSAria cell sorter (BD Biosciences).

Quantitative real-time PCR

Tissues and sorted cells were homogenized in Trizol (Thermo Fisher Scientific) and stored at -80°C. RNA was extracted with chloroform and RNA concentration was determined using a Nanodrop 2000 spectrophotometer (Thermo Fisher Scientific). Reverse transcription of total RNA was performed using the High Capacity cDNA Reverse Transcription kit according to the protocol provided by the manufacturer (Thermo Fisher Scientific). Reaction was detected on a QuantStudio 6 Flex Real-Time PCR (Thermo Fisher Scientific) using the following TaqMan Gene Expression Assays (Applied Biosystems): *Nmu* (Mm00479868_m1), *Nmur1* (Mm00515885_m1), *Nmur2* (Mm00600704_m1) for mouse and *NMU* (Hs00183624_m1), *NMUR1* (Hs00173804_m1) for human samples. Gene expression was normalized as n-fold difference to the gene *Hprt1* (Mm00446968_m1) for mouse and *HPRT1* (Hs02800695_m1) for human samples according to the cycling threshold. Calculation of mRNA levels was performed with the QuantStudio Real-Time PCR software version 1.0 (Thermo Fisher Scientific).

In vitro stimulation and ELISA

Bulk LPLs or sort-purified ILC2s were incubated in DMEM with high glucose supplemented with 10% FCS, 10 mM Hepes, 1 mM sodium pyruvate, non-essential amino acids, 80 μM 2-Mercaptoethanol, 2 mM Glutamine, 100 U/ml Penicillin and 100 μg/ml Streptomycin (all from Gibco) in 96-well microtiter plates (Corning) for 4h at 37°C and 5% CO_2. Neuromedin U-23 (Phoenix Pharmaceuticals or Alpha Diagnostics) or a control peptide (Alpha Diagnostics) were added at 0.1 (Fig, 2 e, f, h), 1 μg/ml (Fig, 2 a-c, g, i,) or 10 μg/ml (Fig, 2 j-o) if not otherwise indicated. If indicated, the culture was supplemented with phorbol 12-myristate 13-acetate (PMA, 1 μg/ml) and ionomycin (Sigma-Aldrich, 1 μg/ml), IL-2, IL-7, IL-33 (R&D, 100 ng/ml, each) and/or IL-25 (eBioscience, 100 ng/ml). The inhibitor of Gαq proteins FR900359 was purified at the University of Bonn and used at 1 μM concentration. In experiments in which intracellular cytokine staining was performed, brefeldin A was added (Sigma-Aldrich, 10 μg/ml).

Cytokines in the supernatant were detected with a sandwich ELISA using IL-5 (TRFK5) or IL-13 (eBio13a) as capture antibodies and IL-5 (TRFK4) or IL-13 (eBio1316H) as detection

antibodies (all from eBioscience) or the Legendplex bead-based assay (Biolegend) for IL-5, IL-9 and IL-13 according to the manufacture's protocol.

Helminth infection

Third-stage larvae (L3) of *N. brasiliensis* were purified with a Baermann apparatus. After washing three times in PBS, living worms were counted. 500 purified larvae were injected subcutaneously in PBS. In addition, in some experiments PBS or NMU (20 μg, Phoenix Pharmaceuticals) was injected i.p. on day 2, 4, and 6 of infection. At day 7 of infection, mice were killed and analyzed if not otherwise indicated. For *T. muris* infection, 200 embryonated eggs were administered by oral gavage. At day 18, a piece from the proximal colon was removed and cleaned in PBS, after which RNA was extracted for qPCR. For *H. polygyrus*, 250 infective L3 larvae were administered by oral gavage. At day 18, a piece from the duodenum was removed and cleaned in PBS, after which RNA was extracted for qPCR.

RNA-seq analysis

For the RNA-seq data presented in Figure 1 ILC2 (Lin^- $CD45^+$ $CD90^+$ $CD127^+$ $KLRG1^+$) and ILC3 (Lin^- $CD45^+$ $CD90^+$ $CD127^+$ $CCR6^+$) lymphocytes were sort-purified from the small intestine of C57BL76 mice. For the RNA-seq data presented in Figure 3 PBS or NMU (20 μg, Phoenix Pharmaceuticals) was injected into $Id2^{Gfp/+}$ mice. After one day, ILC2s from the small intestine were sort-purified as Lin^- $CD45^+$ ID2 GFP^+ $CD127^+$ $CD25^+$ $KLRG1^+$ lymphocytes in Trizol and stored at -80°C. RNA was extracted by using chloroform and further purification with the RNAeasy mini spin columns (Qiagen). RNA samples with an average RNA integrity number (RIN) of 7.9 were further processed.

Sorted cells were used to prepare RNAseq libraries by the Epigenomics Core at Weill Cornell Medicine using the Clontech SMARTer® Ultra® Low Input RNA Kit V4 (Clontech Laboratories). Sequencing was performed on an Illumina HiSeq 2500, yielding 50 bp single-end reads.

Raw sequencing reads were demultiplexed with Illumina's CASAVA (v1.8.2). Adapters were trimmed from reads using FLEXBAR (v2.4)[33] and reads were aligned to the NCBI GRCm38/mm10 mouse genome using the STAR aligner (v2.3.0)[34] with default settings. Reads per gene were counted using Rsubread[35]. One sample was removed from the analysis, as its library size was anomalously small compared to those of the other samples. Genes with at least 10 counts in each sample were considered for further analysis. Differential expression was assessed using DESeq2 version 1.14.0 with default parameters and with a false discovery rate (FDR) of 0.1[36]. Principal component analysis was performed after using DESeq2's variance stabilizing transformation. GO and KEGG term enrichment analysis of differentially expressed genes was performed using the goana and kegga functions of the limma R package[37]. Enrichment p values were then Bonferroni-corrected.

NMU-induced inflammation

NMU (20 μg) or sterile PBS was intranasally administered in a total volume of 30 μl daily. Administration was either performed for 5 days and mice were analyzed after 3 days rest, or analyzed on day 5 after 4 days of administration.

Generation of bone marrow chimeras

Mice were irradiated with 11 Gy from an X-ray irradiator split in two doses of 5.5 Gy and a 4h break between the two cycles. For mixed bone marrow chimeras CD45.1 mice were reconstituted with a 1:1 mixture of full bone marrow from CD45.1 *Nmur1*$^{+/+}$ and CD45.2 *Nmur1*$^{-/-}$ mice. For bone marrow chimeras C57BL/6 mice were reconstituted with either *Nmur1*$^{+/+}$ or *Nmur1*$^{-/-}$ bone marrow. Antibiotics (Sulfamethoxazol and Trimethoprim) were delivered for 2 weeks after bone marrow transplantation in the drinking water and mice were reconstituted for at least 6 weeks before experimentation.

Reconstitution of *Rag2*$^{-/-}$ *Il2rg*$^{-/-}$ mice

Bones were cleaned, washed in 70% EtOH and subsequently in PBS and crushed using a pestle. Bones were rinsed with PBS and bone marrow was resuspended in PBS and filtered through a 70 μM cell strainer. Red blood cells were lysed using ACK buffer (Lonza) and lineage-positive cells were depleted using the Dynabeads untouched mouse CD4 cells kit according to the manufacture's protocol (Thermo Fisher Scientific). Remaining cells were stained and ILC2ps were sort-purified as Lin^{-} Sca-1^{high} CD127^{+} CD25^{+} cells [14]. 1×10^{4} sort-purified ILC2ps were injected i.v. and mice were used at least 4 weeks after adoptive transfer.

Clarity imaging and immunofluorescence

CLARITY imaging was performed following a modified protocol of *Chung et al.* [38]. Briefly, mice were killed and transcardially perfused with 20 ml of ice-cold PBS followed by hydrogel solution combining 1% acrylamide (40%, BioRad), 0.025% bis-acrylamide (2%, BioRad), 0.25% VA-044 initiator (Wako) and 4% PFA in PBS. Intestines were immediately excised, opened longitudinally and cleaned. Tissue was placed in a 50 mL conical tube including 20 ml of cold hydrogel solution and incubated slowly shaking at 4°C for 2 days. The tube was degassed in a desiccation chamber to replace air with nitrogen gas and submerged in a 37°C water bath for 4h until polymerization of the hydrogel solution. Tissue was extracted and cleaned of excess gel followed by washing in clearing solution (200 mM Boric Acid, 4% Sodium Dodecyl Sulfate (pH 8.5; both Sigma-Aldrich) at 37°C on a shaker. Clearing solution was changed every 2 days until tissue became transparent. Tissue was washed twice for 24h in 0.1% Triton X-100 in PBS and stained with indicated antibodies.

For whole mount staining small intestine was cleaned, opened longitudinally and washed ice-cold HBSS with 5% FCS and HBSS with 1 mM DTT. The muscularis mucosa was then mechanically separated form the mucosa by using forceps and washed ice-cold HBSS with 5% FCS. The tissue was fixed in 4% PFA for 2h at room temperature. Afterwards the tissue was washed in ice-cold PBS and blocked with PBS 0.1% Triton X-100 and 10% serum and stained. The following antibodies were used: Rabbit anti-NMU (Santa Cruz), chicken anti-TH (Abcam), mouse anti-SNAP25 (SMI 81, Biolegend), rat anti-CD3ε (17A2, Biolegend), hamster anti-KLRG1 (2F1, eBioscience) followed by goat anti-rabbit Alexa 488, donkey anti-rabbit Alexa 647, goat anti-chicken Alexa 555, goat anti-hamster Alexa 546 (all Thermo Fisher Scientific), donkey anti-rat Alexa 647 (Jackson Immune Research), and images of representative tissue were captured under a LSM 880 confocal microscope and analyzed with Zen software (Zeiss). Surface reconstruction was performed by using Imaris software

(Bitplane). For quantification of ILC2-neuron co-localization we performed background subtraction, and Gaussian smoothing. Then a surface was created and small objects were filtered out for the CD3ε channel. Afterwards, the KLRG1 channel was masked with CD3ε objects in order to remove these from the KLRG1 channel. Background subtraction, Gaussian smoothing, creation of surface and filtering of small objects were performed for KLRG1 channel. This mask was used to select pixels in the NMU channel that overlap with KLRG1. For the masked NMU channel, a surface was created and small objects were filtered out. The objects with and without overlap of the KLRG1 and NMU channel were manually counted.

Enteric neuron culture

Neurosphere culture and differentiation was essentially carried out as described before[39]. In brief, the intestine were dissected from embryos approximately 18 days p.c., minced and washed four times in HBSS/2% FBS (4 min, at 400g). Tissue was digested for 15 min at 37°C in HBSS supplemented with 0.05% Trypsin-EDTA solution (Gibco) and 50 μg/ml DNaseI. After digestion the solution was vortexed and filtered through a 70 μM cell strainer. Cells were plated on an ultralow adherent plate (Corning) in DMEM/F12 supplemented with N2 and Antibiotic-Antimycotic solution (all Gibco) and expanded for 4-5 days. EGF and FGF (20 ng/ml, both R&D) were added to the culture. For differentiation, cells were plated on a 96-well flat-bottom adherent plate (Corning) coated with fibronectin (20 μg/ml in PBS, Sigma) in Neurobasal medium supplemented with B27 and Antibiotic-Antimycotic solution (all Gibco) for 15 days. For co-culture, sort-purified ILC2s were added to the culture with IL-2 and IL-7 (20 ng/ml each).

Human tissues

Human tissues were obtained through an approved research protocol and material transfer agreement with LiveOnNY as described before[40]. Donors were tested to be HIV-, Hepatitis B-, Hepatitis C-negative and did not have chronic disease or cancer. This work does not qualify as‘human subject’research as confirmed by the institutional review board of Columbia University. Tissues were collected after the donor organs were flushed with preservation solution. The intestinal tissue, was washed in PBS, cleaned from fat tissues and cut in smaller pieces, which were incubated in HBSS supplemented with 10 mM Hepes, 5 mM EDTA and 1 mM DTT for 1h at 37°C in a shaking incubator. The specimens were vortexed and filtered through a cell strainer. Epithelium and intraepithelial lymphocytes (IELs) were purified with a 20%/40% Percoll gradient. Digestion solution (collagenase D, Roche, 2 mg/ml), trypsin inhibitor (Thermo Fisher, 1 mg/ml), and DNaseI (0.1 mg/ml) in RPMI medium (Corning), was injected submucosally into the remaining tissue pieces. After incubation at 37°C for 30 min, the samples were chopped and moved to shaking incubator for another 30 min at 37°C. Afterwards, specimens were vortexed, filtered through a tissue sieve and purified over a 40%/80% Percoll gradient. Recovered LPLs were stained with fluorescent-label coupled antibodies and sort-purified. In addition, RNA was extracted from fractioned epithelium, intraepithelial lymphocytes, lamina propria lymphocytes, remaining parenchyma or whole unfractionated tissue using Trizol.

Statistical analysis

P value of mouse data sets was determined by paired or unpaired two-tailed Student's t-test with 95% confidence interval. Normal distribution was assumed. If equal variances between two groups could not be assumed, Welch's correction was performed. Data from human samples were analyzed using a two-tailed Mann-Whitney test with 95% confidence interval. All statistical tests were performed with Graph Pad Prism V7 software. (*p <0.05; **p <0.01 and ***p <0.001; n.s., not significant).

Extended Data

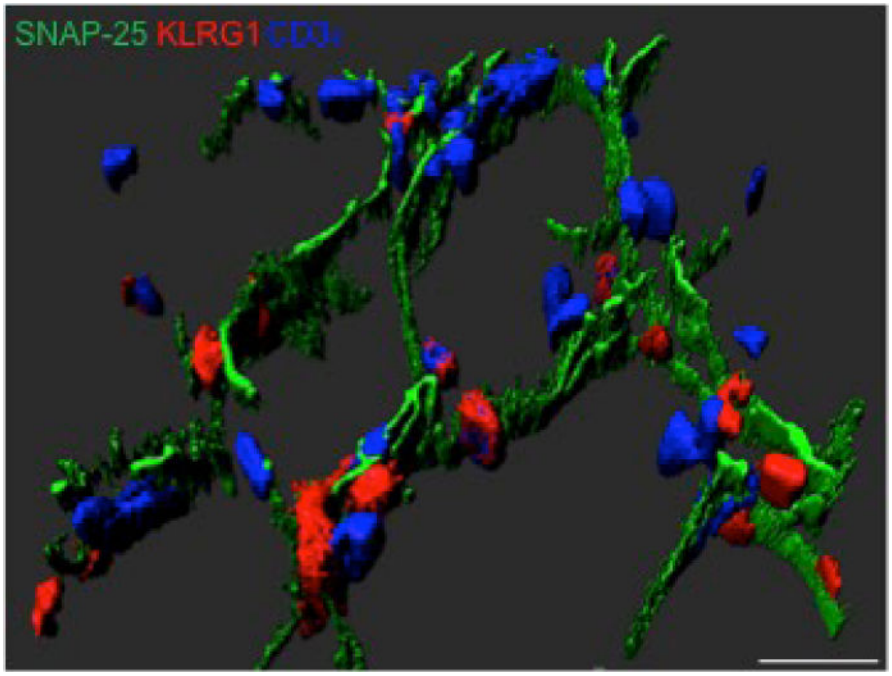

Figure 1. ILC2s and neurons co-localize

Surface reconstruction of immunofluorescent staining from the intestinal submucosa shown in Fig. 1a. Scale bar 30 μm.

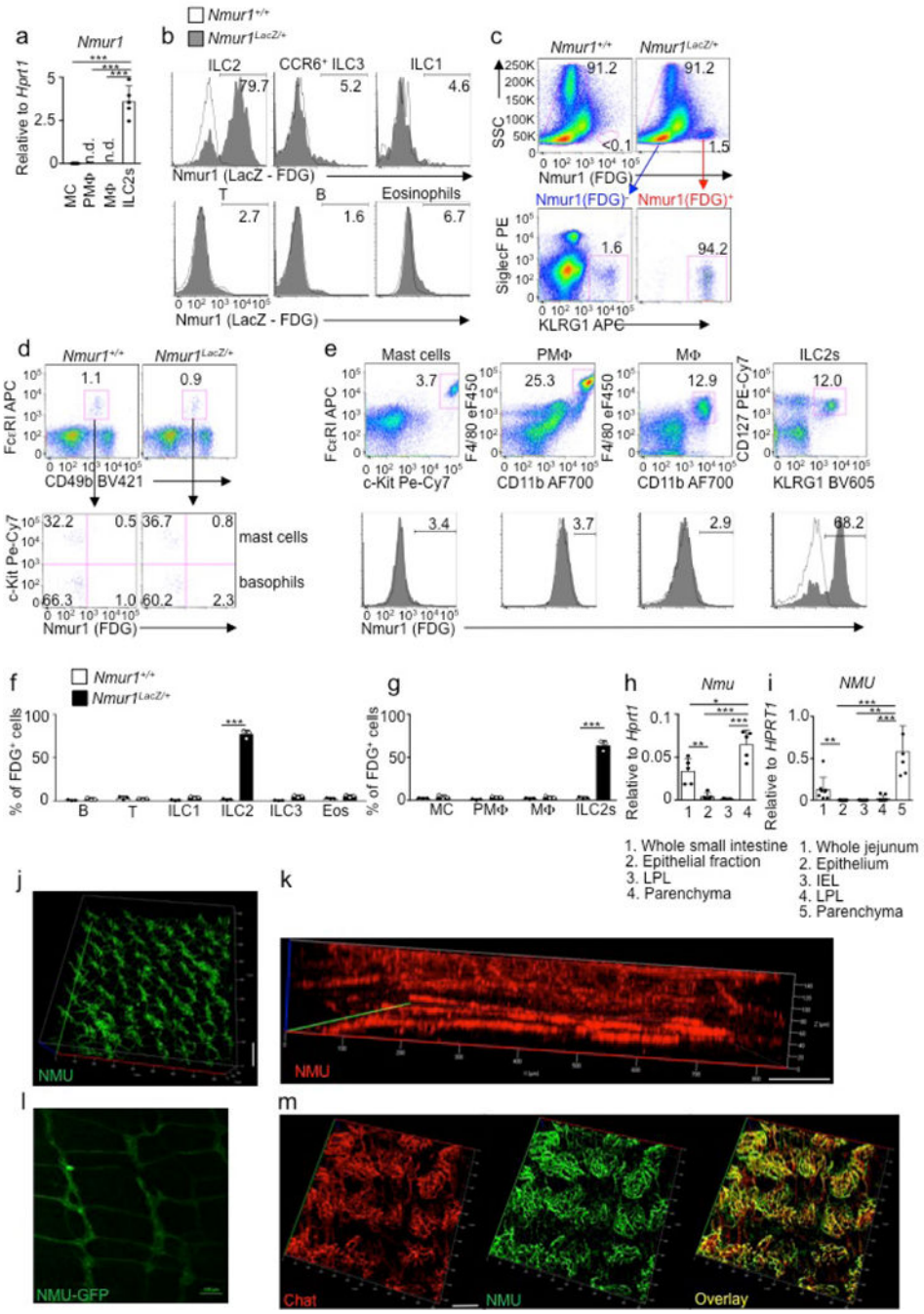

Figure 2. ILC2s selectively express NMUR1

(a) Expression of Nmur1 in the indicated sorted cell populations as determined by qPCR analysis (n = 5). MC, mast cells; MΦ, macrophages; PMΦ, peritoneal macrophages. MC and PMΦ were obtained by peritoneal lavage; MΦ and ILC2s were purified from the small intestine. b–d, f, Histograms and dot plots show expression of Nmur1 as measured by conversion of the fluorescent LacZ substrate FDG. Histograms are gated on Lin−CD45+ cells and CD127+KLRG1+ (ILC2s), CD127+CCR6+ (ILC3s), CD127+CCR6−NKp46+NK1.1+ (ILC1s), CD3+ (T cells), CD19+ (B cells),

CD3−CD19−CD11b+SiglecF+ (Eosinophils) from the small intestine (b, c). Gating for mast cells and basophils from the lung is shown (d). Percentage (n = 3) of FDG+ cells from the indicated population of the small intestine. Eos, eosinophils (f). e, g, Flow cytometry analysis of the indicated immune cell populations (top row) for Nmur1 (bottom row). MC and PMΦ were obtained by peritoneal lavage; MΦ and ILC2 were purified from the small intestine (e). Percentage (n = 3) of FDG+ cells (g). h, Expression of Nmu (n = 3 (LPL), n = 5 (all others)), as determined by qPCR from the indicated fractions of the murine small intestine. i, Expression of NMU (n = 9 (epithelium), n = 8 (whole jejunum and LPL), n = 7 (IEL), n = 6 (parenchyma)) as determined by qPCR from the indicated fractions of the human jejunum. j, k, CLARITY staining of the small intestine (j) or colon (k) for NMU. l, Image of the intestinal muscularis mucosae from NmuGFP mice. m, Immunofluorescence staining of the intestinal mucosa from Chatcre × Ai14 mice for NMU. Scale bar, 100 μm (j–m). Error bars, mean + s.d. Data are representative of two (e, g) or three independent experiments (b–f, j–m) with similar results. Data in a, h, i are based on the indicated number of biological replicates per group.

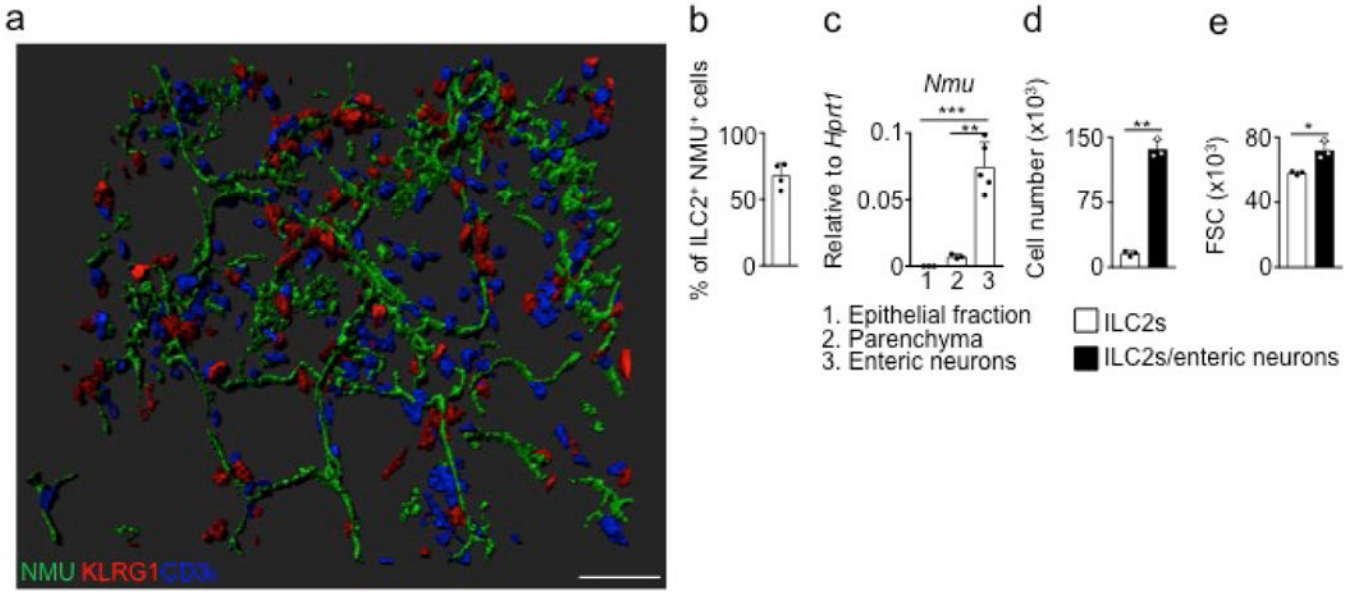

Figure 3. ILC2s and neurons co-localize

(a) Surface reconstruction of immunofluorescent staining from the intestinal submucosa shown Fig. 1i. Scale bar 50 μm.

(b) Percentage (Mean + SD, n= 4) of ILC2s, that have overlapping pixels with neurons. A total of 348 cells were counted and 236 cells exhibited pixels overlapping with NMU staining.

(c) Expression of *Nmu* as determined by qPCR in enteric neuron (Mean + SD, n=5 pooled from two independent experiments) cultures and compared to the epithelial fraction or parenchyma of the small intestine (n=3).

(d,e) Sort-purified ILC2s (3×10^4) were cultured with or without enteric neurons for 5 days. Absolute number (d) and FSC (e) (Mean + SD, n= 3) of ILC2s are shown. Data are representative of three independent experiments.

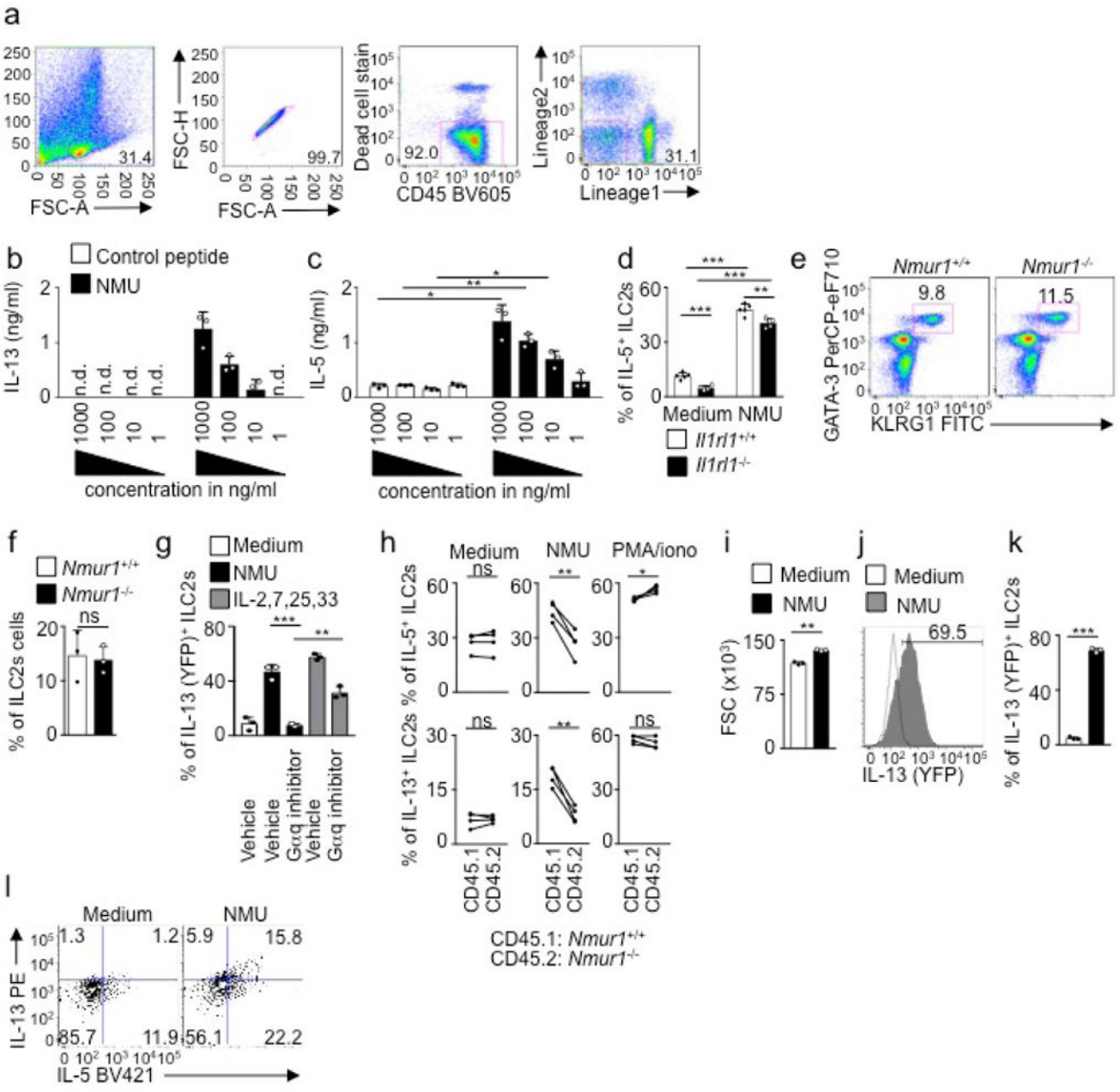

Figure 4. NMU activates ILC2s

(a) Gating strategy for flow cytometric analysis of bulk LPLs cytokine assays. Lineage1: CD11b, CD11c and B220 (all APC-eF780); Lineage2: CD3, CD5 (both PerCP-Cy5.5) and FcεRI PerCP-eF710.

(b,c) Concentration (Mean + SD, n= 3) of IL-13 (b) or IL-5 (c) in the culture supernatant after 4h stimulation of bulk LPLs with a control peptide or NMU as determined by ELISA (n.d. : not detectable).

(d) Bulk LPLs from *Il1rl1*$^{+/+}$ and *Il1rl1*$^{-/-}$ mice were incubated in medium with or without NMU for 4h *in vitro*. Percentage (Mean + SD, *Il1rl1*$^{+/+}$ n= 5, *Il1rl1*$^{-/-}$ n= 4) of IL-5^{+} KLRG1^{+} cells.

(e,f) LPLs from *Nmur1*$^{+/+}$ or *Nmur1*$^{-/-}$ mice were analyzed by flow cytometry. Plots are gated on Lin^{-}CD45^{+} lymphocytes (e). Percentage (Mean + SD, n= 3) of GATA-3^{+} KLRG1^{+} cells (f).

(g) Bulk LPLs were incubated for 30 min with DMSO or the inhibitor of Gαq proteins FR900359 *in vitro*. Medium, NMU or the indicated cytokine cocktail was then added and the assay was incubated for another 4h. Percentage (Mean + SD, n=3) of IL-13 YFP^{+} KLRG1^{+} cells among all KLRG1^{+} cells.

(h) Percentage (Mean + SD, n=4) of IL-5^{+} or IL-13^{+} KLRG1^{+} cells as determined by intracellular cytokine staining.

(j-l) Overnight incubation of sort-purified intestinal ILC2s or C57BL/6 mice (k,l ; n=5).

(i-k) Intestinal ILC2s from *Il13*$^{Yfp/+}$ mice were sort-purified and incubated in medium with or without NMU overnight *in vitro*. FSC (Mean + SD, n=3) (i), histogram overlay of IL-13 YFP (j) and percentage (Mean + SD ; n=3) of IL-13 YFP $^{+}$ ILC2s (k).

(l) ILC2s from the small intestine were sort-purified and incubated in medium without or with NMU over night *in vitro*. Contour plots show intracellular flow cytometry analysis for IL-5 and IL-13.

Data are representative of two (b-d, g,h) or three independent experiments (e, f, i-l) with similar results. Gating in (a) is representative for cytokine assays used in the whole study.

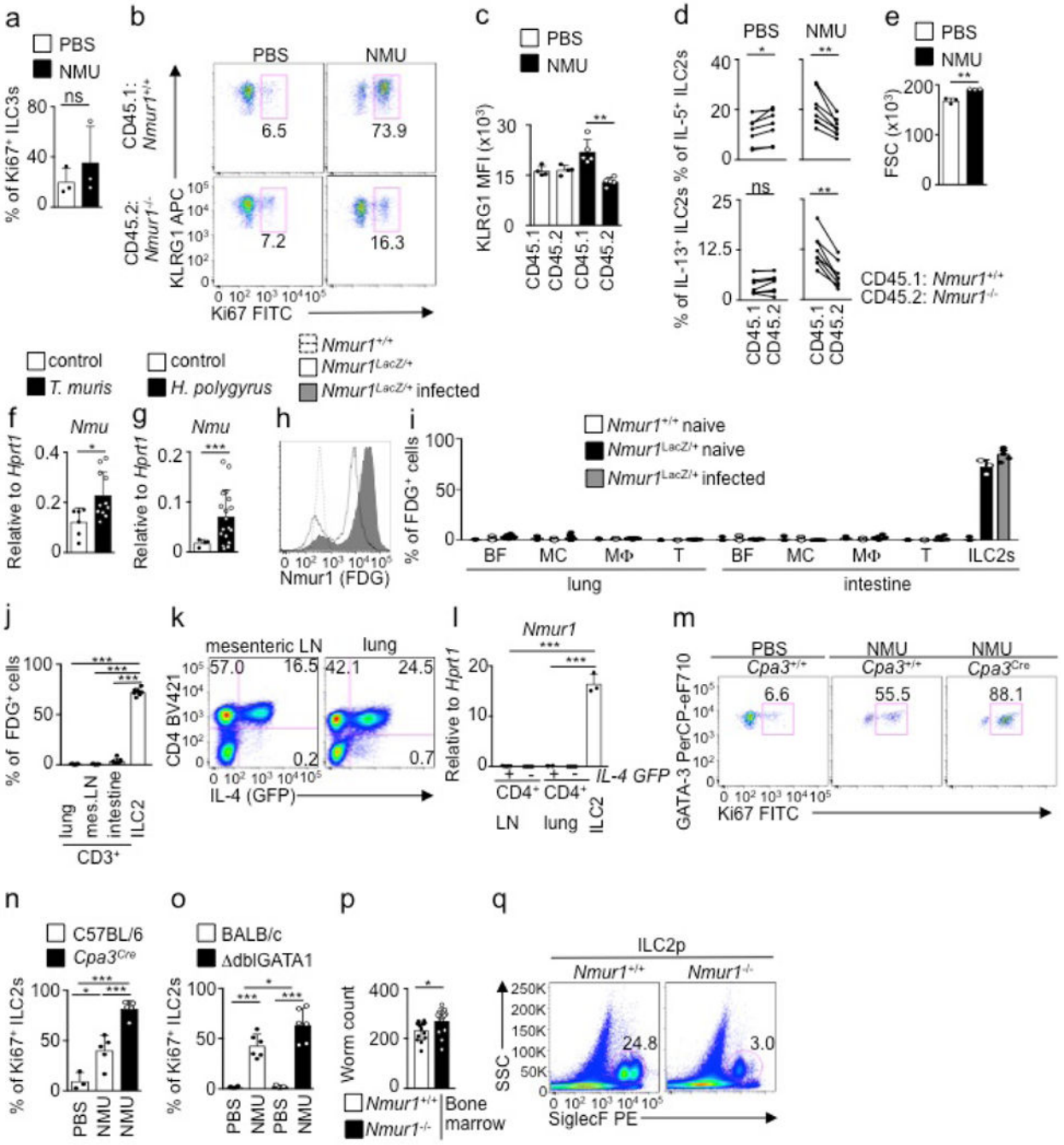

Figure 5. *Nmu* stimulates ILC2s *in vivo*

(a) PBS or NMU was injected daily in C57BL/6 mice. After two days, ILC3s from the small intestine were analyzed by flow cytometry for Ki67. Plots are gated on Lin$^-$ CD45$^+$ RORγt$^+$ lymphocytes. Percentage (Mean + SD, n= 3) of Ki67$^+$ cells.

(b,c) PBS or NMU was injected daily for two days in CD45.1 *Nmur1*$^{+/+}$: CD45.2 *Nmur1*$^{-/-}$ mixed bone marrow chimeras. One day later, ILC2s from the small intestine were analyzed by flow cytometry for KLRG1 and Ki67. Plots are gated on Lin$^-$ CD127$^+$ KLRG1$^+$

lymphocytes and either CD45.1 or CD45.2 (b). KLRG1 MFI (Mean + SD, PBS n=4, NMU n= 5) (c).

(d) PBS or NMU (100 μg) was injected in CD45.1 *Nmur1*$^{+/+}$: CD45.2 *Nmur1*$^{-/-}$ mixed bone marrow chimeras. One day later, ILC2s from the small intestine were analyzed by flow cytometry for IL-5 and IL-13 expression. Percentage (Mean + SD, n= 7) of IL-5^{+} and IL-13^{+} ILC2s. Plots are gated on Lin^{-} CD127^{+} KLRG1^{+} lymphocytes and either CD45.1 or CD45.2.

(e) PBS or NMU was injected once in *Il13*$^{Yfp/+}$ mice. FSC (Mean + SD, n= 3) of Lin^{-} CD45^{+} CD127^{+} CD25^{+} KLRG1^{+} LPLs one day after injection.

(f) C57BL/6 mice were infected with *T. muris* (n=11) or left untreated (n=6). On day 18, *Nmu* expression was determined by qPCR in a piece of the proximal colon.

(g) C57BL/6 mice were infected with *H. polygyrus* (n=18). Control C57BL/6 (n=4) mice were left untreated. On day 18, *Nmu* expression was determined by qPCR in a piece of the duodenum.

(h) *Nmur1*$^{+/+}$ or *Nmur1*$^{LacZ/+}$ mice were infected with *N. brasiliensis.* Control *Nmur1*$^{+/+}$ mice were left untreated. On day 7, mice (n=6) were analyzed. Histogram overlay shows expression of Nmur1 (FDG) on ILC2s from the small intestine and are gated on Lin^{-} CD45^{+} KLRG1^{+} lymphocytes.

(i) *Nmur1*$^{+/+}$ or *Nmur1*$^{LacZ/+}$ mice were infected with *N. brasiliensis.* Control mice were left untreated. On day 7, mice were analyzed and the percentage of Nmur1^{+} (FDG) determined by flow cytometry in the indicated subsets. Percentage (Mean + SD, n= 6 (lung subsets) or 8 (intestinal subsets) for infected *Nmur1*$^{LacZ/+}$ and n= 3 for control mice) of Nmur1^{+} (FDG) cells. Plots are gated on CD45^{+} lymphocytes and FcεRI^{+}CD49b^{+}c-Kit^{-} for basophils, FcεRI^{+}CD49b^{+}c-Kit^{+} for mast cells, CD11b^{+}F4/80^{+} for MΦ, CD3^{+}CD5^{+} for T cells and Lin^{-} KLRG1^{+} for ILC2s.

(j) *Nmur1*$^{LacZ/+}$ mice were infected with *N. brasiliensis.* On day 14, mice were analyzed and the percentage (Mean + SD, n= 7 or 9 (lung)) of Nmur1^{+} (FDG) CD3^{+}CD5^{+} T cells or Lin^{-}KLRG1^{+} ILC2s was determined by flow cytometry.

(k,l) *Il4*^{Gfp} mice were infected with *N. brasiliensis*. On day 14, CD4^{+} T cells (gated on CD3^{+}CD5^{+} lymphocytes) were sort-purified in IL-4 positive and negative populations based on GFP expression (k) and *Nmur1* expression was determined by qPCR (l) (Mean + SD, n=3 (ILC2), n=4 (IL-4^{+} CD4^{+} lung) or n=5).

(m,n) PBS or NMU was injected daily for two days in C57BL/6 or *Xpa3*^{Xpe} mice. One day later, ILC2s from the small intestine were analyzed by flow cytometry for KLRG1 and Ki67 expression. Plots are gated on Lin^{-} CD45^{+} GATA-3^{+} KLRG1^{+} cells (m). Percentage (Mean + SD, n=5 or 3 (PBS)) of Ki67^{+} KLRG1^{+} cells among all KLRG1^{+} cells (n).

(o) PBS or NMU was injected daily for two days in BALB/c or ΔdblGATA1 mice. One day later, ILC2s from the small intestine were analyzed by flow cytometry for KLRG1 and Ki67 expression. Percentage (Mean + SD, n=6 or 5 (PBS ΔdblGATA1) of Ki67^{+} KLRG1^{+} cells among all KLRG1^{+} cells.

(p) Bone marrow chimeras reconstituted with *Nmur1*$^{+/+}$ or *Nmur1*$^{-/-}$ bone marrow were infected s.c. with *N. brasiliensis*. On day 7, worm burden (Mean + SD, n=15) in the small intestine was quantified.

(q) *Rag2*$^{-/-}$ *Il2rg*$^{-/-}$ mice were reconstituted with ILC2 precursors from *Nmur1*$^{+/+}$ or *Nmur1*$^{-/-}$ mice. After reconstitution, mice were infected with *N. brasiliensis* and NMU

(20μg) was injected i.p. on day 2, 4 and 6. Plots show flow cytometry analysis of cells from the lung and are gated on CD45$^+$ CD11c$^-$ cells.

Data are representative of two (b, c, j-q) or three independent experiments (a, e, h) with similar results and n=3-5 mice per group. The experiments in d, f, g, i are pooled data from two (d) or three (f, g, i) independent experiments.

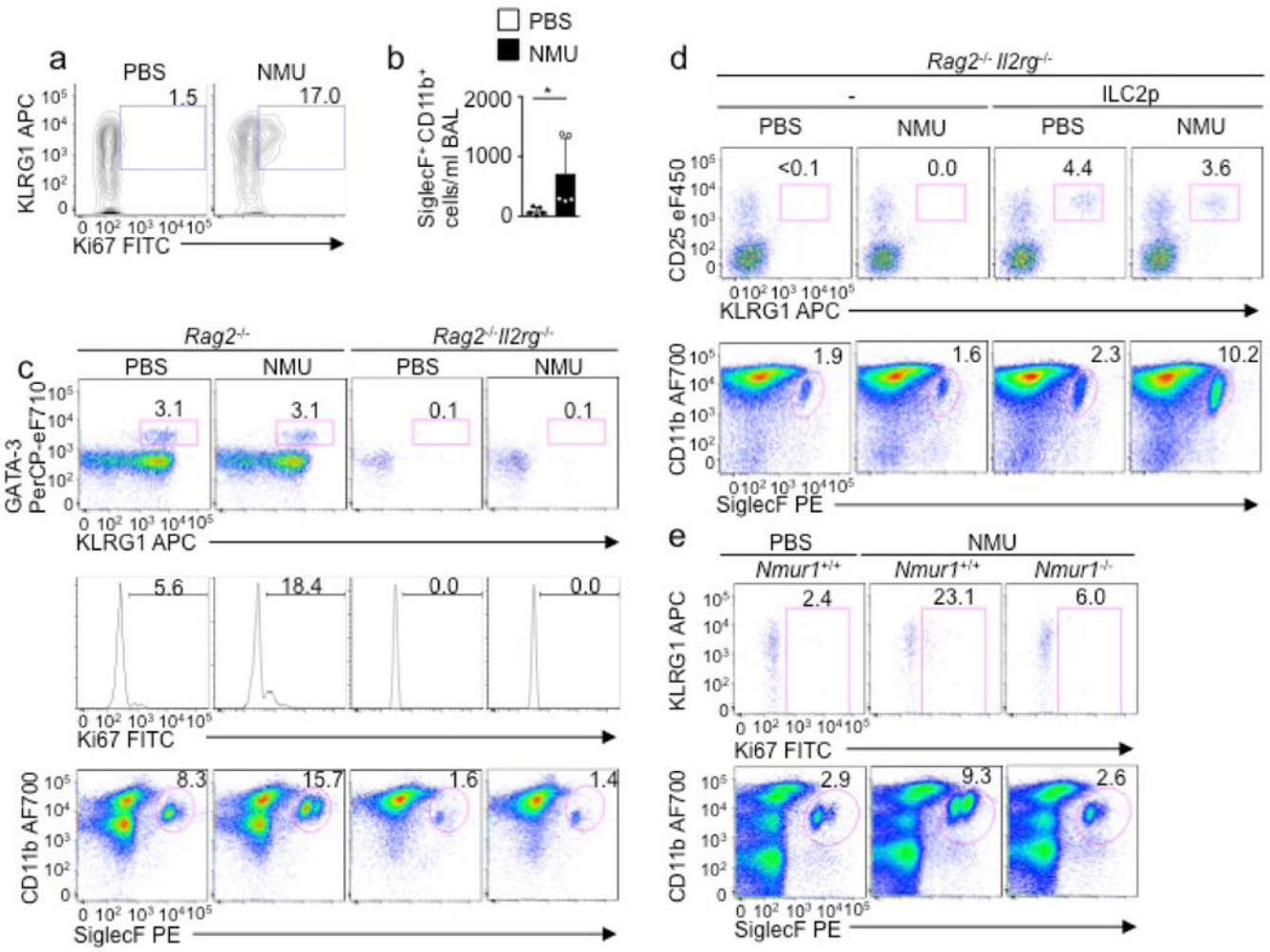

Figure 6. ILC2 are required for NMU-induced lung inflammation

(a) PBS or NMU was intranasally administered to C57BL/6 mice daily for four days. One day later, ILC2s from the lung were analyzed by flow cytometry. Plots are gated on Lin $^-$CD45$^+$ GATA-3$^+$ CD25$^+$ lymphocytes.

(b) PBS or NMU was delivered intranasally to C57BL/6 mice daily for five days. Three days later, eosinophil infiltration was determined in BAL by flow cytometry. Percentage (Mean + SD, n= 5) of CD11b$^+$ SiglecF$^+$ CD11c$^-$ eosinophils in the BAL.

(c) PBS or NMU was intranasally administered to *Rag2*$^{-/-}$ or *Rag2*$^{-/-}$ *Il2rg*$^{-/-}$ mice daily for four days. One day later, ILC2s and eosinophils from the lung were analyzed by flow cytometry.

(d) PBS or NMU was intranasally administered daily for four days to *Rag2*$^{-/-}$ *Il2rg*$^{-/-}$ mice or *Rag2*$^{-/-}$ *Il2rg*$^{-/-}$ that were reconstituted with ILC2ps. One day later, ILC2s and eosinophils from the lung were analyzed by flow cytometry.
(e) PBS or NMU was intranasally administered to *Nmur1*$^{+/+}$ or *Nmur1*$^{-/-}$ mice daily for four days. One day later, ILC2s and eosinophils from the lung were analyzed by flow cytometry. Plots are gated on Lin^{-} CD45^{+} CD25^{+} GATA-3^{+} lymphocytes.
Data are representative of two (d,e) or three independent experiments (a-c) with similar results.

Supplementary Material

Refer to Web version on PubMed Central for supplementary material.

Acknowledgments

We thank I. Gabanyi and D. Mucida for help with the muscularis isolation, H-R Rodewald for providing *Cpa3*^{Cre} and G. Eberl for RORγt^{Gfp} mice. We thank the Epigenomics Core, the Imaging Core and the Mouse Genetics Core at Weill Cornell Medicine and MSKCC. *Nmur1*$^{LacZ/+}$ mice were generated by Velocigene and *Nmu*^{Gfp} by GENSAT and provided by the KOMP or MMRRC Repository at UC Davis. The work was supported by grants from the German Research Foundation (DFG; KL 2963/1-1 to C.S.N.K.; FOR2372 to E.K. and G.M.K.), the Australian National Health and Medical Research Comission (NHMRC) early career fellowship (to L.C.R.), the Novo Nordic Foundation (14052; to J.B.M.), the Weill Cornell Department of Medicine Pre-Career Award (to L.A.M.), the Naito Foundation (to S.M.), JSPS Overseas Research Fellowships (to S.M.), Defense Advanced Research Projects Agency (DARPA; HR0011-16-C-0138 to X.S.), the National Institutes of Health (NIH; AI061570, AI087990, AI074878, AI083480, AI095466, AI095608, AI102942, AI106697 and AI097333 to D.A.; R01GM114254 and OT2-OD023849 to X.S.; AI106697 to D.L.F.), the Burroughs Wellcome Fund (to D.A.) and the Crohn's & Colitis Foundation of America (to T.M and D.A.).

References

1. Pulendran B, Artis D. New paradigms in type 2 immunity. Science. 2012; 337:431–435. DOI: 10.1126/science.1221064 [PubMed: 22837519]
2. Hammad H, Lambrecht BN. Barrier Epithelial Cells and the Control of Type 2 Immunity. Immunity. 2015; 43:29–40. DOI: 10.1016/j.immuni.2015.07.007 [PubMed: 26200011]
3. Locksley RM. Asthma and allergic inflammation. Cell. 2010; 140:777–783. DOI: 10.1016/j.cell.2010.03.004 [PubMed: 20303868]
4. Spits H, et al. Innate lymphoid cells - a proposal for uniform nomenclature. Nature reviews Immunology. 2013; 13:145–149. DOI: 10.1038/nri3365
5. Artis D, Spits H. The biology of innate lymphoid cells. Nature. 2015; 517:293–301. DOI: 10.1038/nature14189 [PubMed: 25592534]
6. Robinette ML, et al. Transcriptional programs define molecular characteristics of innate lymphoid cell classes and subsets. Nature immunology. 2015; 16:306–317. DOI: 10.1038/ni.3094 [PubMed: 25621825]
7. Diefenbach A, Colonna M, Koyasu S. Development, differentiation, and diversity of innate lymphoid cells. Immunity. 2014; 41:354–365. DOI: 10.1016/j.immuni.2014.09.005 [PubMed: 25238093]
8. Walker JA, Barlow JL, McKenzie AN. Innate lymphoid cells - how did we miss them? Nature reviews Immunology. 2013; 13:75–87. DOI: 10.1038/nri3349
9. Klose CS, Artis D. Innate lymphoid cells as regulators of immunity, inflammation and tissue homeostasis. Nature immunology. 2016; 17:765–774. DOI: 10.1038/ni.3489 [PubMed: 27328006]
10. Howard AD, et al. Identification of receptors for neuromedin U and its role in feeding. Nature. 2000; 406:70–74. DOI: 10.1038/35017610 [PubMed: 10894543]

11. Brighton PJ, Szekeres PG, Willars GB. Neuromedin U and its receptors: structure, function, and physiological roles. Pharmacological reviews. 2004; 56:231–248. DOI: 10.1124/pr.56.2.3 [PubMed: 15169928]
12. Veiga-Fernandes H, Mucida D. Neuro-Immune Interactions at Barrier Surfaces. Cell. 2016; 165:801–811. DOI: 10.1016/j.cell.2016.04.041 [PubMed: 27153494]
13. Gautron L, et al. Neuronal and nonneuronal cholinergic structures in the mouse gastrointestinal tract and spleen. The Journal of comparative neurology. 2013; 521:3741–3767. DOI: 10.1002/cne.23376 [PubMed: 23749724]
14. Hoyler T, et al. The Transcription Factor GATA-3 Controls Cell Fate and Maintenance of Type 2 Innate Lymphoid Cells. Immunity. 2012; 37:634–648. DOI: 10.1016/j.immuni.2012.06.020 [PubMed: 23063333]
15. Moriyama M, et al. The neuropeptide neuromedin U promotes inflammation by direct activation of mast cells. The Journal of experimental medicine. 2005; 202:217–224. DOI: 10.1084/jem.20050248 [PubMed: 16009716]
16. Hanada R, et al. Neuromedin U has a novel anorexigenic effect independent of the leptin signaling pathway. Nature medicine. 2004; 10:1067–1073. DOI: 10.1038/nm1106
17. Price AE, et al. Systemically dispersed innate IL-13-expressing cells in type 2 immunity. Proceedings of the National Academy of Sciences of the United States of America. 2010; 107:11489–11494. [PubMed: 20534524]
18. Halim TY, Krauss RH, Sun AC, Takei F. Lung natural helper cells are a critical source of Th2 cell-type cytokines in protease allergen-induced airway inflammation. Immunity. 2012; 36:451–463. DOI: 10.1016/j.immuni.2011.12.020 [PubMed: 22425247]
19. Mjosberg JM, et al. Human IL-25- and IL-33-responsive type 2 innate lymphoid cells are defined by expression of CRTH2 and CD161. Nature immunology. 2011; 12:1055–1062. DOI: 10.1038/ni.2104 [PubMed: 21909091]
20. Monticelli LA, et al. Innate lymphoid cells promote lung-tissue homeostasis after infection with influenza virus. Nature immunology. 2011; 12:1045–1054. DOI: 10.1031/ni.2131 [PubMed: 21946417]
21. Schrage R, et al. The experimental power of FR900359 to study Gq-regulated biological processes. Nature communications. 2015; 6
22. Neill DR, et al. Nuocytes represent a new innate effector leukocyte that mediates type-2 immunity. Nature. 2010; 464:1367–1370. [PubMed: 20200518]
23. Moro K, et al. Innate production of T(H)2 cytokines by adipose tissue-associated c-Kit(+)Sca-1(+) lymphoid cells. Nature. 2010; 463:540–544. [PubMed: 20023630]
24. Moriyama M, et al. The neuropeptide neuromedin U activates eosinophils and is involved in allergen-induced eosinophilia. American journal of physiology Lung cellular and molecular physiology. 2006; 290:L971–977. DOI: 10.1152/ajplung.00345.2005 [PubMed: 16373672]
25. Tallini YN, et al. BAC transgenic mice express enhanced green fluorescent protein in central and peripheral cholinergic neurons. Physiological genomics. 2006; 27:391–397. DOI: 10.1152/physiolgenomics.00092.2006 [PubMed: 16940431]
26. Rossi J, et al. Melanocortin-4 receptors expressed by cholinergic neurons regulate energy balance and glucose homeostasis. Cell metabolism. 2011; 13:195–204. DOI: 10.1016/j.cmet.2011.01.010 [PubMed: 21284986]
27. Madisen L, et al. A robust and high-throughput Cre reporting and characterization system for the whole mouse brain. Nature neuroscience. 2010; 13:133–140. DOI: 10.1038/nn.2467 [PubMed: 20023653]
28. Rawlins EL, Clark CP, Xue Y, Hogan BL. The Id2+ distal tip lung epithelium contains individual multipotent embryonic progenitor cells. Development. 2009; 136:3741–3745. [PubMed: 19855016]
29. Mohrs M, Shinkai K, Mohrs K, Locksley RM. Analysis of type 2 immunity in vivo with a bicistronic IL-4 reporter. Immunity. 2001; 15:303–311. [PubMed: 11520464]
30. Yu C, et al. Targeted deletion of a high-affinity GATA-binding site in the GATA-1 promoter leads to selective loss of the eosinophil lineage in vivo. The Journal of experimental medicine. 2002; 195:1387–1395. [PubMed: 12045237]

31. Feyerabend TB, et al. Cre-mediated cell ablation contests mast cell contribution in models of antibody- and T cell-mediated autoimmunity. Immunity. 2011; 35:832–844. DOI: 10.1016/j.immuni.2011.09.015 [PubMed: 22101159]
32. Hsu CL, Neilsen CV, Bryce PJ. IL-33 is produced by mast cells and regulates IgE-dependent inflammation. PloS one. 2010; 5:e11944. [PubMed: 20689814]
33. Dodt M, Roehr JT, Ahmed R, Dieterich C. FLEXBAR-Flexible Barcode and Adapter Processing for Next-Generation Sequencing Platforms. Biology. 2012; 1:895–905. DOI: 10.3390/biology1030895 [PubMed: 24832523]
34. Dobin A, et al. STAR: ultrafast universal RNA-seq aligner. Bioinformatics. 2013; 29:15–21. DOI: 10.1093/bioinformatics/bts635 [PubMed: 23104886]
35. Liao Y, Smyth GK, Shi W. The Subread aligner: fast, accurate and scalable read mapping by seed-and-vote. Nucleic acids research. 2013; 41:e108. [PubMed: 23558742]
36. Love MI, Huber W, Anders S. Moderated estimation of fold change and dispersion for RNA-seq data with DESeq2. Genome biology. 2014; 15:550. [PubMed: 25516281]
37. Ritchie ME, et al. Limma powers differential expression analyses for RNA-sequencing and microarray studies. Nucleic acids research. 2015; 43 doi:Artn E47.
38. Chung K, et al. Structural and molecular interrogation of intact biological systems. Nature. 2013; 497:332–337. DOI: 10.1038/nature12107 [PubMed: 23575631]
39. Gabanyi I, et al. Neuro-immune Interactions Drive Tissue Programming in Intestinal Macrophages. Cell. 2016; 164:378–391. DOI: 10.1016/j.cell.2015.12.023 [PubMed: 26777404]
40. Tait Wojno ED, et al. The prostaglandin D2 receptor CRTH2 regulates accumulation of group 2 innate lymphoid cells in the inflamed lung. Mucosal immunology. 2015; 8:1313–1323. DOI: 10.1038/mi.2015.21 [PubMed: 25850654]

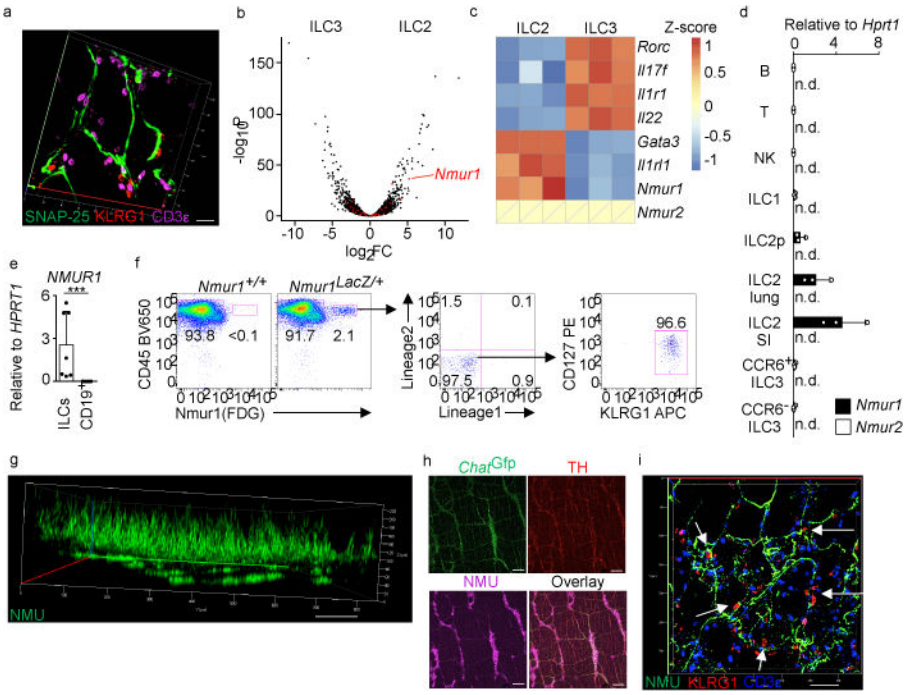

Figure 1. A network of Neuromedin U-expressing neurons co-localizes with NMUR1$^+$ ILC2s

(a) Immunofluorescence staining of the intestinal submucosa. Scale bar 20 μM.

(b) RNA-seq volcano plot of differential expression between ILC2s (positive $\log_2$FC) and ILC3s (negative $\log_2$FC). Genes belonging to the KEGG pathway 'neuroactive receptor-ligand interaction' (mmu04080) are shown in red and are enriched among the genes differentially expressed in ILC2s (corrected p value < 0.01). FC: fold change.

(c) Heatmap showing expression Z-scores of the indicated genes in small intestine ILC2s and ILC3s, as measured by RNA-seq. For *Nmur2*, Z-scores of 0 indicate read counts of zero in all samples.

(d) Expression of *Nmur1* and *Nmur2* in the indicated sort-purified lymphocyte populations as determined by qPCR analysis (Mean + SD, n=3). SI: small intestine; ILC2p: ILC2 progenitor; n.d. : not detectable .

(e) Expression of *NMUR1* in the indicated sorted lymphocyte populations from human intestine as determined by qPCR analysis (Mean + SD, n=7).

(f) Dot plots show expression of Nmur1 as measured by conversion of the fluorescent LacZ substrate fluorescein di-β-D-galactopyranoside (FDG). Lineage1: CD11b, CD11c and B220 (all APC-eF780); Lineage2: CD3, CD5 (both PerCP-Cy5.5) and FcεRI PerCP-eF710.

(g) CLARITY staining of the small intestine. Scale bar 100 μM.

(h) Immunofluorescence staining of the intestinal muscularis mucosae. Scale bar 100 μM.

(i) Immunofluorescence staining of the intestinal submucosa. Scale bar 50 μM.

Data in a and f-i are representative of three independent experiments with similar results. Experiments in b-f are based on three (b-d) or seven (e) biological replicates per group.

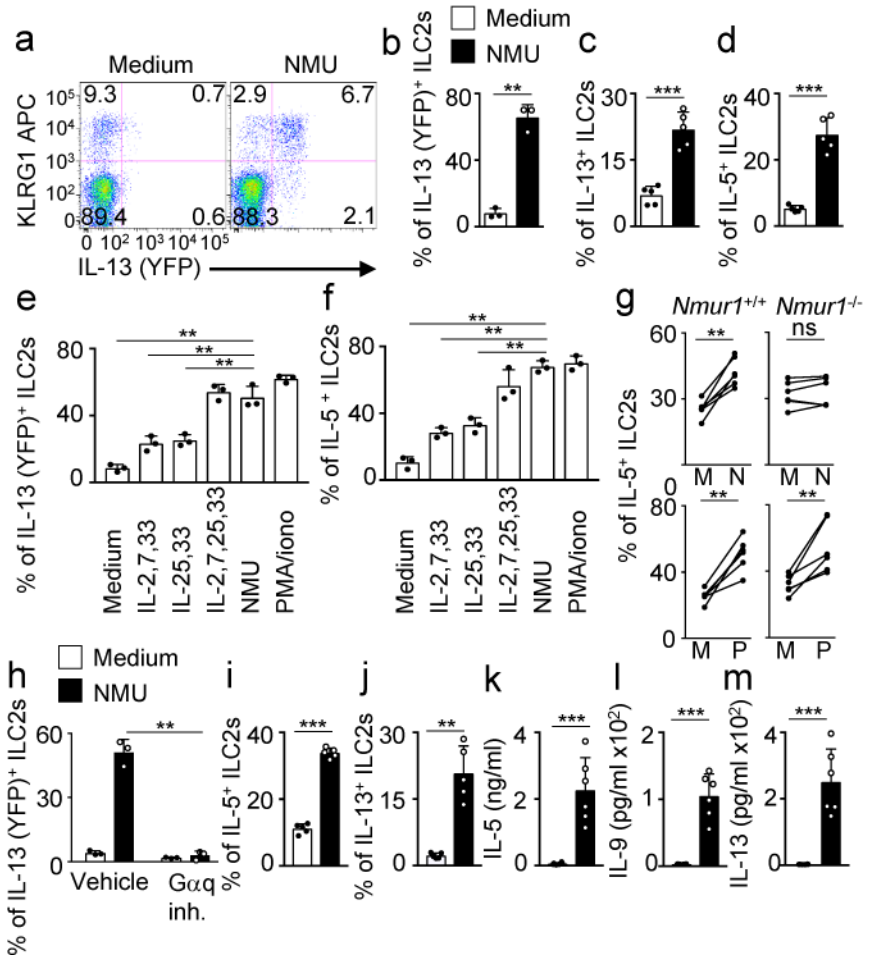

Figure 2. NMU stimulates ILC2s and activates a signaling pathway through NMUR1 and Gαq

Bulk LPLs were incubated in medium without or with NMU and/or the indicated molecules for 4 h *in vitro*.

(a,b) Representative flow cytometry analysis (a). Percentage (Mean + SD, n= 3) of IL-13 YFP$^+$ KLRG1$^+$ cells (b). Gating is shown in ED 4a.

(c,d) Percentage (Mean + SD, n=5) of IL-13$^+$ (c) or IL-5$^+$ (d) KLRG1$^+$ cells as determined by intracellular cytokine staining.

(e,f) Percentage (Mean + SD, n= 3) of IL-13 YFP$^+$ (e) or IL-5$^+$ (f) KLRG1$^+$ cells.

(g) Percentage (Mean + SD, n=6) of IL-5$^+$ KLRG1$^+$ cells. M: Medium; N: NMU; P: PMA/ionomycin.

(h) Bulk LPLs were incubated for 30 min with DMSO or the inhibitor of Gαq proteins FR900359 before incubation with medium or NMU. Percentage (Mean + SD, n=3) of IL-13 YFP$^+$ KLRG1$^+$ cells.

(i,j) Overnight incubation of sort-purified intestinal ILC2s. Percentage (Mean + SD; n=5) of IL-5$^+$ (i) and IL-13$^+$ (j) ILC2s.

(k-m) 7 days incubation of sort-purified intestinal ILC2s. Concentration (Mean + SD, n=6) of IL-5 (k), IL-9 (l), IL-13 (m) in the supernatant.

Data are representative of three (a-f, h-j) independent experiments with similar results. The data in g and k-l are pooled data from two independent experiments and representative for a total of four independent experiments.

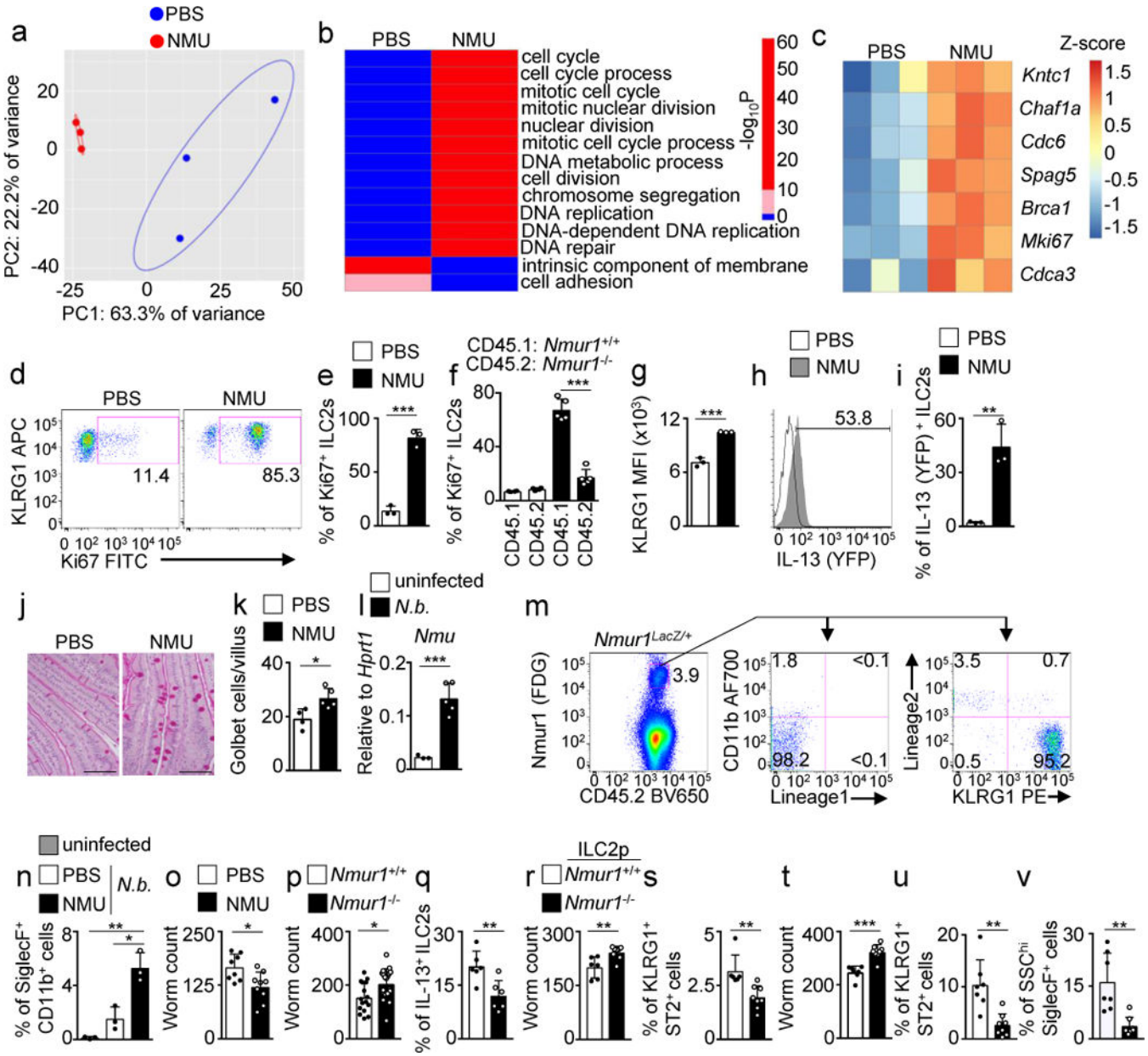

Figure 3. NMU stimulates ILC2s *in vivo* and promotes worm expulsion

(a-c) RNA was extracted from sort-purified ILC2s one day after PBS or NMU administration and sequenced (n= 3). Principal component (PC) analysis. Ellipses show, for each group, the curve at which the fitted bivariate normal distribution equals 0.68 (a). Heatmap showing level of significance of GO enrichment tests, as measured by $-\log_{10}(p_{corrected})$. Blue = not significant ($p_{corrected} > 0.01$) (b). Heatmap showing expression Z-scores of selected differentially expressed genes between PBS- or NMU-treated mice (c). (d,e,f) PBS or NMU was injected daily for two days in C57BL/6 mice (d,e) or in CD45.1 *Nmur1*$^{+/+}$: CD45.2 *Nmur1*$^{-/-}$ chimeras (f). One day later, ILC2s from the small intestine were analyzed by flow cytometry for KLRG1 and Ki67 expression. Plots are gated on Lin^{-}

CD45$^+$ CD25$^+$ KLRG1$^+$ lymphocytes (d). Percentage (Mean + SD, n= 3 (e), n=4 (PBS) n=5 (NMU) (f)) of Ki67$^+$ KLRG1$^+$ cells (e,f).

(g-i) PBS or NMU was injected in *Il13*$^{Yfp/+}$ mice. MFI of KLRG1 expression (g). Histogram overlay for IL-13 (h) is gated on Lin$^-$ CD45$^+$ CD127$^+$ CD25$^+$ KLRG1$^+$ lymphocytes and percentage (Mean + SD, n= 3) of IL-13 YFP$^+$ KLRG1$^+$ cells among all KLRG1$^+$ cells (i) one day after injection.

(j,k) PAS staining after PBS or NMU administration (j). Scale bar 100 μm. Goblet cell number (Mean + SD, n=4 (PBS) n=5 (NMU)) per villus (k).

(l) C57BL/6 mice were infected with *N. brasiliensis* or left untreated. *Nmu* expression was determined by qPCR in the small intestine on day 7 (Mean + SD, uninfected: n= 3, N.b. : Nippostrongylus brasiliensis n=5).

(m) Flow cytometry analysis of Nmur1 (FDG) in LPLs of *N. brasiliensis*-infected *Nmur1*$^{LacZ/+}$ mice. Lineage1: CD11c and B220 (both APC-eF780); Lineage2: CD3, CD5 (both PerCP-Cy5.5).

(n,o) C57BL/6 mice were infected with *N. brasiliensis* and treated with PBS or NMU and analyzed on day 7. Percentage (Mean + SD, n= 3) of CD11b$^+$ SiglecF$^+$ eosinophils in the mesenteric lymph node (n) Worm burden (Mean + SD, PBS n=8, NMU n=9) in the small intestine (o).

(p,q) Worm burden (Mean + SD, *Nmur1*$^{+/+}$ n=16 and *Nmur1*$^{-/-}$ n=19) was determined on day 7 (p) and percentage (Mean + SD, n=6) of IL-13$^+$ ILC2s in the small intestine on day 6 (q).

(r,s) Worm burden (Mean + SD, *Nmur1*$^{+/+}$ n=6, *Nmur1*$^{-/-}$ n=8) of ILC2-reconstituted *Rag2*$^{-/-}$ *Il2rg*$^{-/-}$ mice (r) and percentage of KLRG1$^+$ ST2$^+$ was measured by flow cytometry in the lung (s).

(t-v) Worm burden (Mean + SD, *Nmur1*$^{+/+}$ n=7, *Nmur1*$^{-/-}$ n=8) of ILC2- reconstituted and NMU injected *Rag2*$^{-/-}$ *Il2rg*$^{-/-}$ mice (t) or percentage of KLRG1$^+$ ST2$^+$ (u) or eosinophils (v) was measured by flow cytometry in the lung.

Data are representative of two (q) or three independent experiments (d-m) with similar results. Experiments in (o, q-v) are pooled data from two (q-v) or three (o) independent experiments. RNA-seq data in a-c are based on three biological replicates per group.

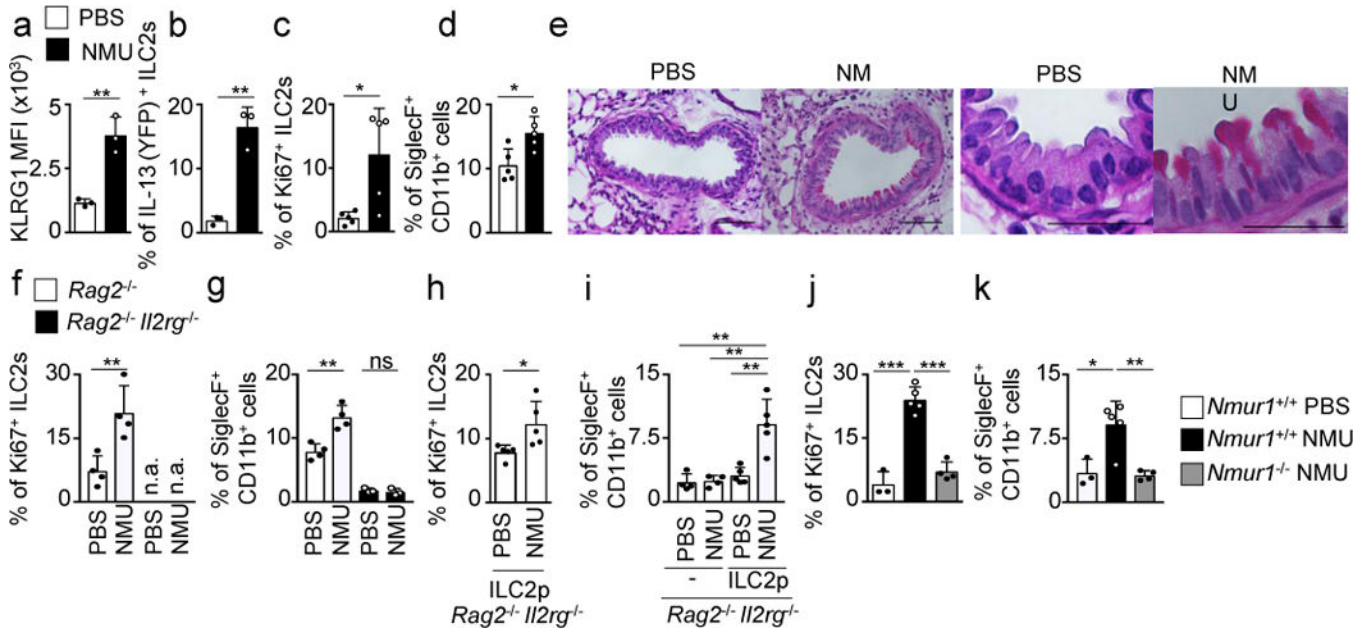

Figure 4. NMU induces ILC2-dependent lung inflammation

(a-c) PBS or NMU was intranasally administered to *Il13*$^{Yfp/+}$ (a,b) or C57BL/6 (c) mice daily for four days. One day later, ILC2s from the lung were analyzed by flow cytometry. MFI (Mean + SD, n= 3) of KLRG1 expression (a). Percentage (Mean + SD, n= 3) of IL-13 YFP^{+} ILC2s (b). Percentage (Mean + SD, n= 5) of Ki67^{+} KLRG1^{+} cells (c).

(d,e) PBS or NMU was delivered intranasally to C57BL/6 mice daily for five days and lung infiltration was examined three days later. Percentage (Mean + SD, n= 5) of CD11b^{+} SiglecF^{+} CD11c^{-} eosinophils in the lung (d). PAS staining of lung sections (left side: scale bar 100 μm; right side: scale bar 50 μm. Electronically magnified images from the left are shown on the right (e).

(f-k) PBS or NMU was intranasally administered to *Rag2*$^{-/-}$ or *Rag2*$^{-/-}$ *Il2rg*$^{-/-}$ mice (f,g), ILC2-reconstituted *Rag2*$^{-/-}$ *Il2rg*$^{-/-}$ mice (h,i), or *Nmur1*$^{+/+}$ or *Nmur1*$^{-/-}$ mice (j,k) for four days. One day later, ILC2s and eosinophils from the lung were analyzed by flow cytometry. Percentage (Mean + SD, n= 4 (f,g), n= 4 (*Rag2*$^{-/-}$ *Il2rg*$^{-/-}$), n=5 (*Rag2*$^{-/-}$ *Il2rg*$^{-/-}$ + ILC2p) (h,i), n=3 (PBS), n=5 (NMU) n=4 (NMU *Nmur1*$^{-/-}$) (j,k) of Ki67^{+} KLRG1^{+} cells (f,h,j) or percentage of CD11b^{+} SiglecF^{+} CD11c^{-}eosinophils (g, i, k) (n.a. : not applicable).

Data are representative of two (h, i) or three independent (a-g and j,k), experiments with similar results.